Global and multiscale features of the magnetosphere: data-derived and global MHD modeling

A. S. Sharma

University of Maryland, Department of Astronomy, College Park, Maryland, USA

Abstract. The Earth's magnetosphere exhibits global features such as plasmoid formation and release, and multiscale behavior, e. g., turbulence, bursty bulk flows, current disruption, etc. It is essential to model these features properly in order to forecast them accurately and efficiently. The global behavior has clear dynamical behavior and can be predicted using dynamical models. The multiscale features on the other hand has a power law behavior and can not be modeled in the dynamical sense and can be described/modeled in terms of statistical properties. These properties of the magnetosphere are modeled using correlated data of the solar wind – magnetosphere coupling and global MHD simulations. The data-derived models yield forecasts of the global behavior from a mean-field model and the statistical limits of predictability from the multiscale features.

Index Terms. Global MHD simulations, nonlinear dynamical techniques, solar wind – magnetospere coupling, space weather forecasting.

1. Introduction

The disturbances originating at the sun can lead to many hazardous effects in the geospace environment, and the development of predictive models of these is one of the key objectives of the International Living With a Star (ILWS) program. The chain of physical processes at the sun and their coupling to the solar wind, the magnetosphere, the ionosphere and the thermosphere, span a wide range of space and time scales and consequently it is at present a challenge to develop a single comprehensive model in which all these processes are directly represented. The present models, such as MHD (global, two-fluid and Hall), hybrid and particle-in-cell simulations each cover a part of the spectrum of processes and new multiscale simulation approaches are needed to cover the global and multiscale phenomena.

The solar wind-magnetosphere coupling has been studied extensively using data from many space missions and modeling approaches. The coupling of the solar wind mass, momentum and energy to the magnetosphere is enhanced when the interplanetary magnetic field (IMF) turns southward, leading to geospace storms and substorms. The magnetosphere is a highly dynamic system under these conditions and its main component, the magnetospheric substorms, are disturbances with a typical time scale of an hour. When the IMF remains southward for an extended interval, the ring current grows under the influence of the solar wind variations, leading to geospace storms with typical time scales of days and are characterized by strong variations in the magnetic field on the ground. Along with the storms and substorms there are a number of processes, e. g., turbulence, bursty bulk flows, current disruption, etc., that contribute to the multiscale phenomena.

The Earth's magnetosphere is a non-autonomous dynamical system, driven by the solar wind. Studies of the magnetospheric dynamics using models derived from the correlated data of the solar wind – magnetosphere system have enhanced our understanding of the complex behavior of the magnetosphere. The advantage of this approach is the ability to yield the dynamical behavior of the system, inherent in observational data, independent of modeling assumptions. There has been considerable progress in the modeling and forecasting of the solar wind-magnetosphere coupling as an input-output system using techniques of nonlinear dynamics and complexity (Sharma et al., 2005). These data-derived models are based on the correlated data of the input time series $I(t)$ (usually the solar wind convective electric field VB_z) and the output time series $O(t)$ (the geomagnetic activity index *AE* or *AL* for substorms and the *Dst* index for storms).

The modeling of magnetospheric substorms as a low dimensional system using the time series data of the auroral electrojet indices, *AL* or *AE*, to reconstruct its dynamics has shown its low dimensionality and therefore its predictability (Sharma, 1995). The data-derived models have been used to provide reliable forecasts of substorms (Vassiliadis et al., 1995; Ukhorskiy et al., 2002) and storms (Valdivia et al., 1996). Recent studies using time series data have shown that the coherence on the global magnetospheric scale can be modeled by averaging over the short scales. This follows from the recognition that the magnetosphere has features which are clearly global, such as during plasmoid formation and release during substorms, and in the same time there are stochastic or multiscale features. A model for the global features has been obtained by using the mean field technique of averaging outputs corresponding to similar states of the

system in the reconstructed phase space (Ukhorskiy et al., 2002, 2004). With such a mean-field model, accurate iterative long-term predictions are readily obtained, and since the model parameters need not be changed during predictions they are suitable for space weather forecasting. This approach is now used to forecast storms and substorms near real time using the solar wind data from ACE spacecraft.

The data-derived models yield reliable and accurate forecasts of geomagnetic activity due mainly to the ability of the nonlinear dynamical techniques in recognizing the inherent features in the data. However these models are empirical in nature and do not identify the physical variables and processes directly. The global MHD models (Lyon, 2000; Gombosi et al., 2003; Raeder, 2003) are based on the first principles and provide a framework for developing a comprehensive model of solar wind-magnetosphere coupling.

Considering the strong forecasting capabilities of data-derived models and the potential of the first principle models to develop into comprehensive models, it is important to characterize their common elements. This will yield an understanding of the manner in which these models complement each other and clarify the future directions for the development of improved models. This paper presents a comparison of the global and multiscale behavior in these models based on the data-derived modeling using the Bargatze et al. (1985) database and the global MHD simulations for the same dataset.

2. Data-derived modeling of the magnetosphere

Recognizing the driven nature of the magnetosphere, the solar wind – magnetosphere coupling is modeled as an input-output system. The local-linear filters (Ukhorskiy et al., 2002) use the dynamical characteristics of the solar wind (input) to model the geomagnetic activity (output). In this approach the dynamical behavior of the magnetosphere is obtained directly from observational data, and have the advantage of being unencumbered by presumed processes.

The magnetosphere has been shown to exhibit the features of a nonlinear dynamical system, and its global features have been modeled by a small number of variables (Sharma, 1995). This remarkable property arises from the inherent property of phase space contraction in dissipative nonlinear systems. A dynamical input-output model can be constructed based on local-linear filters, which represent the relationship between the input *I(t)* and the output *O(t)*. It is assumed here that the time series data contain the information necessary to determine the system evolution. When the phase space is reconstructed properly the evolution of the system can be modeled without any loss of dynamical characteristics inherent in the data. Such a data-derived model can then be used to predict the future states of the dynamical system.

The time delay embedding technique is an appropriate method for the reconstruction of the phase space and for obtaining its characteristic properties. In this technique, an m-component phase vector X_i is constructed from the time series *x(t)* as:

$$X_i = \{x_1(t_i), x_2(t_i), \cdots, x_m(t_i)\}, \quad (1)$$

where $x_k(t_i) = x(t_i + (k-1)T)$ and T is a time delay.

In an input-output model of the solar wind-magnetosphere system during substorms, the solar wind convective electric field VB_s (V being the solar wind speed and B_s the southward component of the IMF) is commonly used as the input and the geomagnetic activity index *AL* or *AE* as the output. Thus the input-output vector in the m dimensional embedding space can be constructed as

$$X_i = (I_1(t_i), I_2(t_i), \cdots, I_{M_I}(t_i), O_1(t_i), O_2(t_i), \cdots, O_{M_O}(t_i)), \quad (2)$$

where $M_I = M_O = m$. The $2m$-dimensional state vector X_i at t = t_1, t_2, . . . t_N, can now be used to construct a trajectory matrix for the dynamics of the system. This matrix represents the dynamical behavior of the system contained in the data and yields its evolution in the reconstructed phase space.

A. Local-linear and mean field filters

The local-linear filters are widely used to represent the dynamics taking into account the nonlinearity of the system. The main idea of this method is the use of the trajectories in the neighborhood of the state at time t to predict its location at the next time step. From the details of how the neighboring trajectories evolve, the location of the current state *x(t)* at next time step $t+T$ can be predicted. The procedure is locally linear but is essentially nonlinear as the features of the neighboring trajectories are taken into account by considering a small neighborhood. For a given time series, a proper embedding dimension is obtained when two states x_k and x_n, which are close together in the embedded phase space, yield the next states of O_{k+1} and O_{n+1} which are also close together (Ukhorskiy et al., 2002).

The predicted output O_{n+1} can be described as a nonlinear function of the input I_n and current output O_n as

$$O_{n+1} = F(I_n, O_n). \quad (3)$$

In this model the magnetospheric dynamics is represented by a state vector and the function F governing the evolution of the magnetospheric state O_n depends on both the input and the previous states. A Taylor expansion of F up to the linear terms gives:

$$O_{n+1} \approx F^{(0)}(I_n^c, O_n^c) + \sum_{i=0}^{M_I-1} A_i \delta I_{i+1,n} + \sum_{j=0}^{M_O-1} B_j \delta O_{j+1,n}$$
$$= F^{(0)}(I_n^c, O_n^c) + A\delta I_n + B\delta O_n$$

The zero order term $F^{(0)}$ is a function of (I_n^c, O_n^c), the center of expansion, while δO_n and δI_n are small deviations from the center. The three parameters $F^{(0)}, \delta O_n, \delta I_n$ can be obtained from the known data, which is referred to as the training set. Given the current state, the states similar to the

current states in the training set are selected as the first step. The degree of similarity of the current state with any other state in the training set is quantified by the Euclidean distance between them in the embedding space. The states within a specified distance of the current state are referred to as the nearest neighbors.

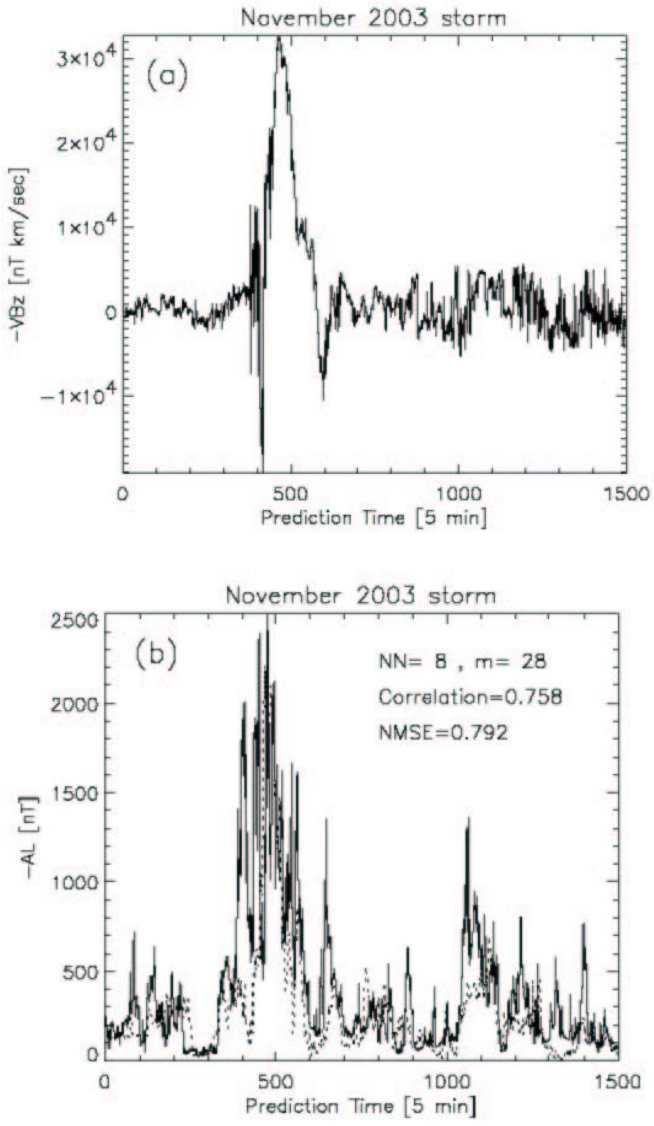

Fig. 1. The weighted mean field predictions for the 2003 November storm. The solar wind input – VB_z, shown in panel (a), has a sudden increase that drives the storm and the substorms. The values of the actual (solid line) and predicted (dash line) values of – AL are shown in panel (b). The values of m and NN correspond to minima in the normalized square error (Chen and Sharma, 2006).

The average value of the state vectors of the nearest neighbors is usually defined as the center of the expansion, referred to as the center of mass, and is used in defining the nonlinear filters for short term and long-term predictions of the auroral electrojet indices (Ukhorskiy et al., 2002). Thus the predicted output is given by

$$O_{n+1} = \langle O_{n+1} \rangle_{NN} + A\delta I_n + B\delta O_n , \qquad (4)$$

in which $\langle O_{n+1} \rangle_{NN} = \frac{1}{NN}\sum_{k=1}^{NN}(\vec{I}_n^k, \vec{O}_n^k)$. Ukhorskiy et al. (2002) pointed out that for a long-term prediction of *AL* time series, the terms other than the center of mass consist of the higher order terms of the filter for local-linear ARMA filter. These terms cannot be modeled in a consistent manner and should be ignored in developing a global model. The prediction procedure then reduces to a search of the average response of the system. In this forecasting method the choice of the nearest neighbors (*NN*) and the embedding dimension (*m*) are critical. If a large number of neighbors is used it is likely to lead to a smoothing of the dynamical variations, while a small number may lead to a wide differences among the chosen states. The choice of the embedding dimension m is based on the unfolding of the dynamics in the reconstructed phase space. For a state X_n, if the dimension *m* and its *NN* nearest neighbors represent the system properly, the average over *NN* nearest neighbors defines the smooth manifold of dimension *m* on which its dynamics can be predicted. Thus the prediction using the mean field approach (Ukhorskiy et al., 2004) is given by

$$O_{n+1} = \frac{1}{NN}\sum_{k=1}^{NN} X_k \qquad (5)$$

The local-linear ARMA and the local-linear mean field filters have been obtained from the correlated database of solar wind and geomagnetic activity time series (Ukhorskiy et al., 2002, 2003, 2004). Both these techniques yield very good results with the small or medium values of the dimension *m*, indicating that the global aspects of the magnetospheric dynamics can be modeled as a low-dimensional system.

B. Weighted mean field filter

In the mean field model all the states in the specified neighborhood, the *NN* nearest neighbors, are used to obtain the center of mass by a simple averaging procedure. It is however expected that the states close to the current state, and thus are similar, should contribute more than those farther away in deciding the predicted state. Based on this recognition, a new filter based on the mean field filter has been proposed to improve the accuracy and efficiency of predictions [*Chen and Sharma*, 2006]. This weighted filter takes into account the distances of the nearest neighbors and thus is not a simple average over the *NN* nearest neighbors. Since some of the nearest neighbors are far way from each other and also farther away from the center of mass, a set of weight factors $\boldsymbol{g}$ can be introduced such that they depend inversely on the distances of each nearest neighbor from the mass center. The weights can thus be chosen to be

$$g_k = \frac{1}{d_k^2} \Big/ \sum_{i=1}^{NN} \frac{1}{d_i^2} , \qquad (6)$$

where d_i is the Euclidean distance of the i^{th} nearest neighbor from the center of mass. Then the predicted output that includes these weighting of the neighbors is

$$O_{n+1} = \frac{1}{NN}\sum_{k=1}^{NN} X_k \bullet g_k \qquad (7)$$

In the limit all the nearest neighbors have the same distance from the center of mass, the weighted mean-field filter will yield the same prediction as the mean field filter. However if the *NN* nearest neighbors are distributed over a wide range of the distances from the center of mass, the nearest neighbors closer to the center of mass will dominate the output of the prediction. The inclusion of nearest neighbors farther away should not affect the prediction significantly as these will have smaller weights, thus making the predictions less sensitive on the number of nearest neighbors *NN*. This weighted mean field filter can capture the large scale features because averaging *NN* nearest neighbors can smooth the high frequency variations.

C. Modeling of superstorms

The weighted mean field filter has been used to model the solar wind-magnetosphere coupling during the superstorms of October-November 2003. The solar wind induced electric field VB_z, which includes both the northward and southward components of IMF, is used as the input. The following steps are adopted in order to obtain the optimal nonlinear weighted mean field filters for superstorms (Chen and Sharma, 2006). First, the activity level of the solar wind driving is computed by averaging the southward component of VB_Z. Then both the input (VB_z) and the output (*AL*) of the time interval corresponding to the same activity level of the magnetosphere from the 2001 database are selected as the training set. For the two superstorms, the selected data group from the 2001 database is the "super" level ($\langle VB_S \rangle \geq 2500$ nT·km/s) of the database. Second, using the selected data interval of input VB_Z and its corresponding *AL* as a training set, the index *AL* is predicted for the superstorms using the weighted mean field filter. The normalized mean square error (NMSE) is used to determine the optimal parameters for the prediction by comparing the predicted and actual *AL* values. In this model, three free parameters can be used to minimize the NMSE. The first two parameters are the embedding dimensions M_I and M_o. However $m = M_O = M_I$ in general and consequently the vector length in the phase space is *2m*. The third parameter is the number of nearest neighbors *NN*. From a wide range of values of these parameters a small set of values are chosen by examining the NMSE's for a range of *m* and *NN* (Chen and Sharma, 2006). The solar wind convective electric filed ($-VB_Z$) for the November 2003 storm, shown in Fig. 1(a), shows a sudden enhancement in the early part of the event and this drives the geospace storm. The predicted and real *AL* are shown in Fig. 1(b). The solid line represents the real *AL* and the dashed line represents the predicted *AL*. Iterative predictions of the November 2003 storm were carried out for 7500 minutes (125 hours) with a minimum NMSE of 0.792 and maximum correlation coefficient of 0.758. In the predictions shown in Fig. 1, the output closely reproduces the sharp variations of *AL* and captures some of the abrupt changes.

Earlier prediction studies (e.g., Vassiliadis et al., 1995; Ukhorskiy et al., 2002, 2004) used Bargatze et al. (1985) dataset, which corresponds to the declining phase of a solar cycle and contains only a few weak storms with *Dst* < -25 nT, and substorms with *AL* values of –1000 nT. On the other hand, the superstorms of November 2003 occurred close to the last solar maximum and the storm intensities were extremely high, with a *Dst* value of - 472 nT and a *AL* value of – 2499 nT. Since such storms are uncommon, it is naturally hard to find many similar events in the available databases, such as that of year 2001. So the nearest neighbor searches in these cases yield only a few states close to that of the superstorms. If we use a large number of nearest neighbors and a simple arithmetic averaging over them, the output of the model is smoothed over these and cannot capture the peaks of the substorms. In such cases the weight factor $\boldsymbol{g}$ plays an important role and yields improved predictions (Chen and Sharma, 2006).

3. Global and multi-scale phenomena

The predictability of the magnetosphere demonstrated by using the data-derived models has two important implications. First, it shows the global coherence of the magnetosphere in terms of the low-dimensionality of the system (Vassiliadis et al., 1990; Sharma, 1995). This feature is consistent with the global picture obtained from the theory, modeling and observations (Siscoe, 1991), and from the global MHD simulations (Lyon, 2000). Second, the predictive ability of the data-derived models is high, and has provided reliable tools for space weather forecasting.

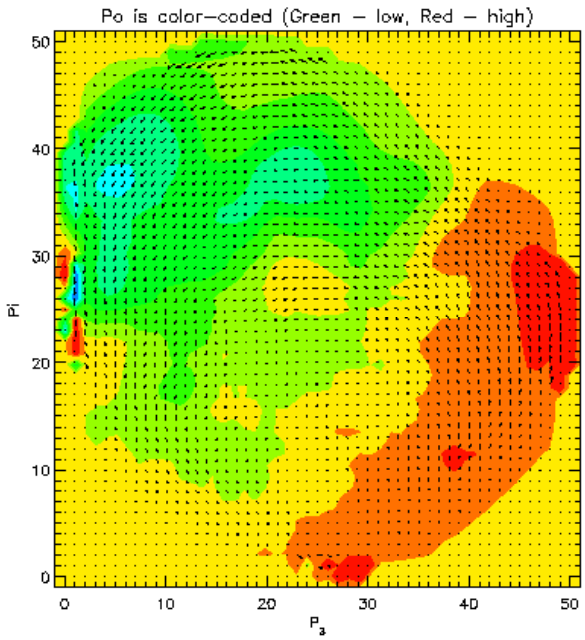

Fig. 2. The dynamical manifold of the trajectories in the three dimensional space (the first three components) obtained from the singular spectrum analysis of the correlated data of the coupled solar wind – magnetosphere. The arrows are the flow vectors and show the trajectories making the transition from the elevated (red) to the lower (green) region (Sitnov et al, 2000).

In the nonlinear dynamical sense the global coherence or low-dimensionality implies that the trajectories of the magnetosphere lie on a surface or manifold and it would be

possible to obtain a representation of this surface by using suitable techniques. The technique of singular spectrum analysis has been used successfully to obtain the dynamical behavior of the magnetosphere (Sharma et al., 1993). This technique essentially identifies the leading variables of a system in terms of the eigenvalues and eigenfunctions of the covariance matrix derived from the trajectory matrix discussed in Sec. 2. The singular eigenvalues and eigenfunctions computed from the time series data provide an ordered set of orthonormal vectors inherent in the data and are suitable for further studies of the dynamical behavior. For example, in the case of dynamical systems whose time series data is contaminated with noise, this technique yields the leading variables as the eigenvalues above a noise level.

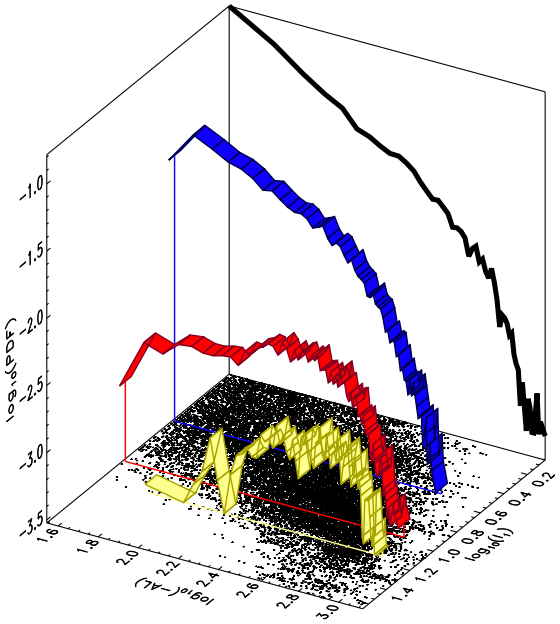

Fig. 3. The conditional probabilities of *AL* index as functions of the solar wind VB_s. The strong driving (yellow) leads to a more global response (peaked) whereas the weak driving leads to a Power-law distribution of AL index with no dominant scale. The black curve is the marginal distribution and the entire data set represented by the points on the floor (Ukhorskiy et al., 2004).

The magnetospheric dynamics, being driven by the turbulent solar wind, is complex and most of the techniques developed for dynamical systems can not be applied readily. The singular spectrum analysis has been adapted to analyze the correlated database of the coupled solar wind – magnetosphere system to yield the simplest representation of the surface generated by the dynamical trajectories (Sitnov et al., 2000), shown in Fig. 2. The red region shows the 'higher" level from which the system evolves to the "lower" level shown in yellow. The arrows show the flow vectors of the dynamical trajectories.

The multiscale features of the magnetosphere are evident in many studies of the power law spectra obtained from observational data. The principle components of the dynamics obtained from the singular spectrum analysis can be used to analyze the distribution of scales in the magnetospheric response to the solar wind driving. The magnetospheric resonse (*AL* index) for a given level of solar wind input (VB_z) can be used to compute the conditional probabilities, which in turn can be used to study the dependence of the former to the latter in a Bayesian manner. The magnetospheric response can be different for different levels of driving by the solar wind. In order to study such differences in the conditional probabilities, the VB_s in Bargatze et al. (1985) database is divided into three activity levels: strong (VB_s > 9 mV), medium (0.6 < VB_s < 9 mV) and weak (VB_s < 0.6 mV). The conditional probability $P(O_{t+1}, x_t)$ is defined in the embedding space x_t for the predicted output O_{t+1} (Ukhorskiy et al., 2004). The probability distributions are shown in Fig. 3 for the different activity levels: strong (yellow), medium (red) and weak (blue). The conditional probabilities for the entire data set is given by the black curve in the back panel of Fig. 3 and the floor shows all the points in the database.

The conditional probabilities of the magnetospheric response to the different levels of driving by the solar wind show significant dependence on the latter. For the weak activity (blue ribbon in Fig. 3), the distribution is essentially a combination of two power law distributions. This reflects the multiscale nature of the magnetosphere in which there is no dominant scale in the response. On the other hand the medium (red) and strong (yellow) activity levels have similar distributions, with peaked distributions with a sharper peak for the latter, and reflect the dominance by the global magnetospheric dynamics. The marginal probability distribution corresponding to the entire data set is essentially scale-free, with a break in the spectrum at $-AL \sim 500$ nT.

From the forecasting point of view it is important to recognize the differences in the magnetospheric response for different solar wind conditions. In order to improve the accuracy in the forecasts of the magnetospheric state, the first step is to identify the intensity of the solar wind variations and then find similar events in the past. These events form the database for modeling and forecasting the ensuing disturbances.

4. Global MHD simulations of the magnetosphere

The interaction of a time varying solar wind with the magnetosphere has been modeled extensively using a 3-D MHD code coupled interactively with a 2-D electrostatic, height integrated ionospheric model. It usually consists of two tightly coupled modules (Fedder and Lyon, 1995). The first module is a 3D MHD that simulates the solar wind-magnetosphere interaction on a logically spherical grid deformed to be nearly cylindrical, typically with radius 100 R_E and length over 400 R_E. The computational grid is designed to place maximum resolution at critical locations, such as the bow shock, magnetopause, and tail plasma sheet. Solar wind conditions are maintained along the sunward and side edges of the computational grid thereby allowing use of time dependent solar wind parameters from spacecraft, such as WIND and ACE, as input conditions. A simple supersonic

outflow condition is used at the far tail boundary, x = -450 R_E. The second module models the response of the ionosphere, and provides the inner boundary condition on the MHD module. This module is a height integrated electrostatic model that solves Poisson's equation, $\nabla E \nabla \Phi = J_{\parallel}$, where Φ is the ionospheric potential, E the conductance tensor and $J_{\parallel}$ the field aligned current. The conductance tensor has both Pedersen and Hall components, whose values are spatially varying with prescriptions dependent on the electron precipitation and the solar ultraviolet radiation. The ionospheric model is coupled to the inner boundary of the MHD module, located typically at 2-3 R_E by line tying matching conditions. The electron precipitation and $J_{\parallel}$ inputs to the ionospheric module are computed from the MHD module. In turn the electric potential computed in the ionospheric module is input on the inner boundary of the MHD module. The LFM global magnetospheric model (Lyon, 2000) is driven by measured solar wind parameters and completely specifies the polar plasma convection patterns and strength as well as the ionospheric auroral conductance.

The LFM global MHD model was used to simulate the magnetosphere during selected intervals of Bargatze et al. (1985) dataset. The solar wind conditions are obtained from the IMP8 satellite database for 7 intervals in the medium activity level. These intervals have a total duration of around 280 hours and are characterized statistically by simple input-output relationships. Also these intervals are suitable for benchmarking the global MHD simulations. The solar wind variables are the density, velocity, magnetic field and thermal pressure. Thus the simulations use more details of the solar wind than VB_s in the case of Bargatze et al. (1985). As usual the solar wind variables are propagated to the front boundary of the global MHD model. The full ionospheric model is used and the dipole tilt is taken into account in these simulations (Shao et al., 2003).

The simulated magnetospheric and ionospheric response, saved every minute in the SM coordinate system, were used to develop a database of the coupled input-output system as given by the global MHD model. The solar wind input to the MHD code consists of several variables and they can be used as the input variables in the nonlinear dynamical analysis. However, since substorms are closely associated with the southward interplanetary magnetic field, in the analysis of the simulation results the solar wind input is represented by the induced electric field VB_s. Also this allows a better comparison of the data-derived and global MHD models by using the same set of variables.

The pseudo-*AL* index is used as the measure of the magnetospheric response during substorms. In order to emulate the manner in which the actual AL index is computed, the pseudo-*AL* index is derived from the maxima of the westward ionospheric Hall current obtained by a search of the computational grid in the northern hemisphere. The actual *AL* index is derived from the H components of the magnetic field monitored at 12 stations distributed in the auroral region. The deviations of the H component of the magnetic field variations at the different stations from their quiet-time values are plotted together to obtain the *AL* index as the lower envelope. The observational *AL* index is a measure of the strength of the auroral electrojet and is directly proportional to the east-west (azimuthal) ionospheric Hall current or the westward electrojet during magnetospheric substorms. The pseudo-*AL* index, derived from global MHD model, is computed following a procedure similar to that of the actual *AL* index. The relation between the observed *AL* index and the simulated or pseudo-AL index were analyzed in detail. For example, the 16th interval in Bargatze et al. (1985) data set corresponding to May 27-29, 1974 covers about 35 hours and the 24th interval (Aug. 26-27, 1974) in the same data set covers about 40 hours. In both these cases the simulated pseudo-*AL* index is found to tract the observed *AL* index closely on the whole (Shao et al., 2003). The coupled VB_s-pseudo-*AL* index data was analyzed using nonlinear dynamical techniques in the same manner in which Bargatze et al. (1985) were analyzed. This yields a comparison of the dynamical features of the magnetosphere from the MHD simulations with those from the observations.

Using the same techniques as in the data-derived modeling (Sitnov et al., 2000), the principal components P_j (j=1, 2, 3) are obtained from the simulation data and these are used to construct the 3-D surface created by the trajectories. In the first eigenvector the output component (pseudo-AL index) is the dominant one, and the corresponding principal component along this eigenvector is levelled P_o. This variable is closely related to time-averaged output or the magnetospheric response to the solar wind. In the second eigenvector, the input component VB_s is dominant, and the corresponding principal component is leveled P_i , and is closely related to time-averaged input. In the third eigenvector, the variations in the input component is dominant and the corresponding principle component is leveled P_3. Thus P_3 is roughly proportional to the time derivative of the input component. With these three variables the manifold of the magnetospheric dynamics can be obtained, and is shown in Fig. 4. In this figure the principal component P_o is color-coded and the smoothed surface is achieved through a standard triangulation procedure. The circulation flows given by dP_3/dt and dP_o/dt are represented by the arrows. To the lowest order, the surface in Fig. 4 can be approximated by a two-level surface, and closely resembles the manifold in Fig. 2 derived from the observational data. The phase transition-like behavior of substorms, exhibited by Fig. 2, is thus reproduced by the global MHD simulations.

The substorm cycle starts in the region with $P_i = 0$ and $P_3 = 0$ in Fig. 4, and the arrows show the trajectory of the evolution. When P_i increases above zero, P_o remains nearly zero and shows small decreases, while P_3 increases first, then remains nearly constant. This region corresponds to the growth phase in the substorm cycle. Subsequently when P_o takes large negative values the flow arrows are the largest,

and intensifications follow, corresponding to the expansion phase. The system evolves back to the original state with decreases in P_i and $-P_o$. This stage broadly corresponds to the recovery phase of substorms.

The dynamical manifolds shown in Figs. 2 and 4 correspond to the same solar wind conditions and are obtained from the singular spectrum analysis of the actual and simulated magnetospheric responses. The overall agreement between the two leads to the conclusion that the global MHD model reproduces the solar wind – magnetospheric coupling quite well. The visualizations of the simulation results for many specific events show the dynamics of the magnetosphere and the results shown in Figs. 2 and 4 represent a clear statistical comparison of the simulated and observational data. It should also be noted that both figures show that the evolution of the magnetosphere on the global scale is quite regular and resembles the temperature-pressure-density diagram of equilibrium phase transitions in a two phase system, e. g., the water-steam system. The differences in the details in the two cases arise, at least in part, from the inherent multiscale nature of the magnetosphere.

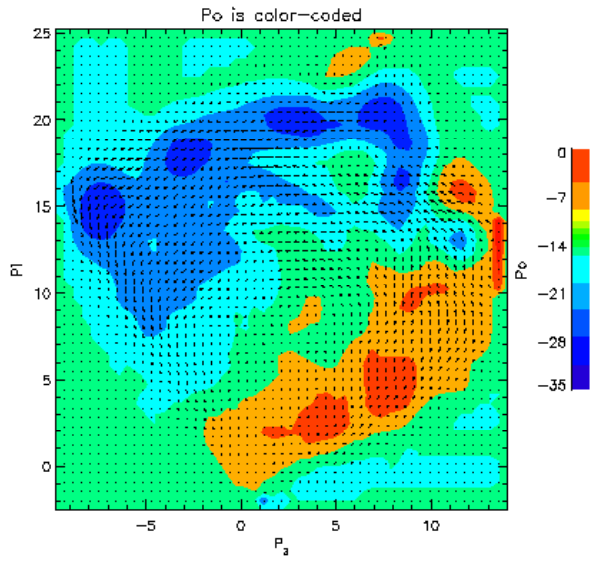

Fig. 4. The two-dimensional approximation of the manifold representing magnetospheric dynamics. The principal component P_3 is color-coded. The circulation flows are given by dP_i/dt and dP_o/dt are represented by arrows. This manifold obtained from the global MHD simulations closely resembles the one obtained from the data-derived modeling (Shao et al., 2003).

The multiscale behavior of the magnetosphere has many origins and has been interpreted as arising from phase transition-like processes, self-organized criticality and turbulence (Sharma et al., 2005b). The singular spectrum analysis of the observational and simulated data yield power law distributions, which indicate a scale-free character. Driven by the turbulent solar wind, the magnetosphere during geomagnetically active periods is far from equilibrium and storms and substorms are essentially nonequilibrium phenomena. The multiscale and intermittent behavior originate, in part, from this nonequilibrium nature. In the phase transition scenario of the magnetospheric global and multiscale behavior, the global features are associated with first order phase transitions and the multiscale features are associated with second-order phase transitions (Sitnov et al., 2000; Sharma et al., 2005a). This scenario, initially based on data-derived modeling, is borne out by the global MHD simulations. This convergence of the data-derived and global MHD models show that these properties are inherent in the magnetosphere.

5. Conclusion

The global and multiscale aspects of the magnetosphere have been recognized for sometime now, but they have been studied separately. The data-derived and global MHD models provide integrated models of these inherent properties of solar wind – magnetosphere coupling.

The data-derived models have been developed from extensive observational data, corresponding to a wide range of different activity levels. For example, Bargatze et al. (1985) database represents a declining phase of the solar activity and Chen and Sharma (2006) is for 2001 during the peak of the last solar maximum. The studies of these geospace disturbances in these data sets by using the techniques of nonlinear dynamics clearly reveal the global and multiscale behavior. Recognizing that the magnetosphere is neither completely low dimensional nor completely stochastic, new forecasting tools have been developed to yield dynamical forecasts of the global features and statistical descriptions of the multiscale features in terms of conditional probabilities (Ukhorskiy et al., 2004). The conditional probabilities are computed as Bayesian measures in the input-output phase space and can be used for risk assessment analysis.

The global MHD model has now emerged as the leading first principles model of the solar wind - magnetosphere coupling and has provided both qualitative and quantitative results advancing our understanding. Most of the global MHD simulations have been of events relevant to particular studies, e. g., of space weather events. The simulations of long periods of the magnetosphere corresponding to the well known Bargatze et al. (1985) data set has provided the basis for the comparison of the data-derived modeling with simulations. The analysis of the simulated data using nonlinear dynamical techniques shows the global and multiscale features of the magnetosphere obtained earlier from data-derived modeling.

The good agreement between the data-derived and global MHD models is a significant advance in our understanding of the magnetospheric dynamics. It shows a confluence in the levels of modeling capabilities. It also shows that the global and multiscale features observed in both models are truly inherent in magnetospheric dynamics.

The global MHD models are large scale simulation models which have been developed over decades and require

extensive resources of supercomputers. The data-derived models on the other hand are considerably simpler models which require workstation level computer resources. The ability of the latter to yield the results at the level of large scale simulations is a testament on the advances in our understanding of complex systems, especially in nature.

Acknowledgments. The author thanks J. Chen, C. Goodrich, P. Guzdar, J. Lyon, K. Papadopoulos, X. Shao, M. Sitnov and A. Ukhorskiy for their contributions to the collaborative research. The research is supported by NSF grants ATM-0318629 and DMS-0417800, and NASA grant NNG04GE37G.

References

L. F. Bargatze, D. N. Baker, R. L. McPherron and E. W. Hones, "Magnetospheric impulse response for many levels of geomagnetic activity", *J. Geophys. Res.*, vol. 90, p. 6387, 1985.

J. Chen and A. S. Sharma, "Modeling and prediction of the magnetospheric dynamics during intense geospace storms", *J. Geophys. Res.*, vol. 111, A04209, doi:10.1029/2005JA011359, 2006.

J. A. Fedder and J. G. Lyon, "The Earth's magnetosphere is 165 R_E long: Self consistent currents, convection, magnetospheric structure, and processes for northward interplanetary magnetic field", *J. Geophys. Res.*, vol. 100, p. 3623, 1995.

T. I. Gombosi, D. L. De Zeeuw, K. G. Powell, A. J. Ridley, I. V. Sokolov, Q. F. Stout and G. Tóth, "Adaptive Mesh Refinement MHD for Global Space Weather Simulations", in *Space Plasma Simulation (Lecture Notes in Physics)*, J. Büchner, C. T. Dum, M. Scholer, Eds., pp. 251-279, Springer, Berlin-Heidelberg-New York, 2003.

J. G. Lyon, "The solar wind-magnetosphere-ionosphere system", *Science*, vol. 288, p. 1987, 2000.

J. Raeder, "Global magnetohydrodynamics – a tutorial", in *Space Plasma Simulation (Lecture Notes in Physics)*, J. Büchner, C. Dum, M. Scholer, Eds., Springer, Berlin-Heidelberg-New York, p. 212, 2003.

X. Shao, P. N. Guzdar, A. S. Sharma, K. Papadopoulos and J. G. Lyon, "Phase transition-like behavior of substroms: Comparison of results from observations and MHD simulations", *J. Geophys. Res.*, vol. 108, p. 1037, doi:10.1029/2001JA009237, 2003.

A. S. Sharma, D. Vassiliadis and K. Papadopoulos, "Reconstruction of low dimensional magnetospheric dynamics by singular spectrum analysis", *Geophys. Res. Lett*., vol. 20, p. 335, 1993.

A. S. Sharma, "Assessing the magnetosphere's nonlinear behavior: Its dimension is low, its predictability, high (US National Report to IUGG, 1991-1994)", *Rev. Geophys. Supple.*, vol. 33, pp. 645-650, 1995.

A. S. Sharma, D. N. Baker and J. E. Borovsky, "Nonequilibrium phenomena in the magnetosphere: Phase transition, self-organized criticality and turbulence", in *Nonequilibrium Phenomena in Plasmas*, A. S. Sharma and P. K. Kaw, Eds., pp. 117-144, Springer, Berlin-Heidelberg-New York, 2005a.

A. S. Sharma, A. Y. Ukhorskiy and M. I. Sitnov, "Global and multiscale phenomena in the magnetosphere", in *Nonequilibrium Phenomena in Plasmas*, A. S. Sharma and P. K. Kaw, Eds., pp. 3-22, Springer, Berlin-Heidelberg-New York, 2005b.

G. Siscoe, "The magnetosphere: A union of interdependent parts", *EOS, Trans. AGU*, vol. 72, p. 494, 1991.

M. I., Sitnov, A. S. Sharma, K. Papadopoulos, D. Vassiliadis, J. A. Valdivia, J. Klimas and D. N. Baker, "Phase transition-like behavior of the magnetosphere during substorms", *J. Geophys. Res*., vol. 105, p. 12295, 2000.

M. I. Sitnov, A. S. Sharma, K. Papadopoulos and D. Vassiliadis, "Modeling substorm dynamics of the magnetosphere: From self-organization and self-organized criticality to nonequilibrium phase transitions", *Phys. Rev. E*., vol. 65, 0161116, 2001.

A. Y. Ukhorskiy, M. I. Sitnov, A. S. Sharma and K. Papadopoulos, "Global and multi-scale properties of magnetospheric dynamics in local-linear filter", *J. Geophys. Res.*, vol. 107, p. 1369, 2002.

A. Y. Ukhorskiy, M. I. Sitnov, A. S. Sharma and K. Papadopoulos, "Combining global and multi-scale features in description of the solar wind-magnetosphere coupling", *Ann. Geophysicae*, vol. 21, p. 1913, 2003.

A. Y. Ukhorskiy, M. I. Sitnov, A. S. Sharma and K. Papadopoulos, "Global and multiscale dynamics of the magnetosphere", *Geophys. Res., Lett.*, vol. 31, L008802, 2004.

J. A. Valdivia, A. S. Sharma and K. Papadopoulos, "Prediction of Magnetic Storms Using Nonlinear Models", *Geophys. Res. Lett.*, vol. 23, p. 2899, 1996.

D. Vassiliadis, A. S. Sharma, T. E. Eastman and K. Papadopulos, "Low Dimensional Chaos in Magnetospheric Activity from Time-Series AE Data", *Geophys. Res. Lett.*, vol. 17, p. 1841, 1990.

D. Vassiliadis, A. J. Klimas, D. N. Baker and D. A. Roberts, "A description of solar wind-magnetosphere coupling based on nonlinear filters", *J. Geophys. Res.*, vol. 100, p. 3495, 1995.